2006

Effect of Ti and metal vacancies on the electronic structure, stability, and dehydrogenation of Na3AlH6: Supercell band-structure formalism and gradient-corrected density-functional theory

S. Li
Virginia Commonwealth University

Puru Jena
Virginia Commonwealth University, pjena@vcu.edu

Li, S., Jena, P., Ahuja, R. Effect of Ti and metal vacancies on the electronic structure, stability, and dehydrogenation of Na3AlH6: Supercell band-structure formalism and gradient-corrected density-functional theory. Physical Review B, 73, 214107 (2006).

Effect of Ti and metal vacancies on the electronic structure, stability, and dehydrogenation of Na_3AlH_6: Supercell band-structure formalism and gradient-corrected density-functional theory

S. Li and P. Jena
Physics Department, Virginia Commonwealth University, Richmond, Virginia 23284-2000, USA

R. Ahuja
Condensed Matter Theory Group, Department of Physics, Uppsala University, Box 530, SE 751 21 Uppsala, Sweden
(Received 21 September 2005; revised manuscript received 7 March 2006; published 9 June 2006)

Electronic and structural properties of sodium-aluminum hexahydride (Na_3AlH_6) formed during the decomposition reaction of sodium alanate ($NaAlH_4$) and the effects of Ti catalyst are studied using supercell approach and density-functional theory. The preferred site of Ti has been determined by substituting it at both the Na and Al sites and comparing the respective formation energies. The least unfavorable site for Ti is found to be the Al site. To examine the role of Ti substitution on the desorption of hydrogen, the energy cost to remove a H atom from the vicinity of Ti was calculated and compared with that from the pure Na_3AlH_6 The improvement in dehydrogenation of Na_3AlH_6 was found to be due to the weakening the Al-H bond caused by Ti substitution. We also studied the role of metal vacancies on hydrogen desorption. Although this desorption was exothermic, the energies to create these vacancies are high.

DOI: 10.1103/PhysRevB.73.214107 PACS number(s): 68.43.Bc, 68.43.Mn, 81.05.Zx, 71.15.Nc

I. INTRODUCTION

Complex light metal hydrides such as alanates ($MAlH_4$, $M=Li,Na$),[1] borohydrides (MBH_4, $M=Li,Na$),[2,3] imides (M_2NH, $M=Li,Na$),[4] and amides (MNH_2, $M=Li,Na$) (Ref. 5) have been the subject of intense investigation in the last five years due to their potential as hydrogen storage materials. However, the desorption of hydrogen from these materials requires rather high temperatures. Thus ways must be found not only to weaken the metal-hydrogen bonds, but also to lower the barrier for hydrogen sorption before these complex hydrides can seriously be considered as hydrogen storage materials for on-board applications.[6] A recent discovery by Bogdanovic and Schwickardi[1] that the addition of a small amount of Ti based catalyst can significantly improve the thermodynamics and reversibility of sodium alanate ($NaAlH_4$) has provided much hope that the complex light metal hydrides may be suitable for practical applications if appropriate catalysts can be found.

We note that the desorption of hydrogen from sodium alanate occurs in three distinct steps[7,8]

$$NaAlH_4 \rightarrow 1/3Na_3AlH_6 + 2/3Al + H_2, \quad (1)$$

$$1/3Na_3AlH_6 \rightarrow NaH + 1/3Al + 1/2H_2, \quad (2)$$

$$NaH \rightarrow Na + 1/2H_2. \quad (3)$$

The first decomposition reaction occurs at 353 K, releasing 3.7 wt % of hydrogen. In the second step, which occurs at 423 K, 1.9 wt % of hydrogen is released. The remaining 1.9 wt % hydrogen, released at 698 K does not have much practical value as the temperature is too high for on-board applications.[9]

Most of the recent experimental and theoretical works have focused exclusively on understanding, from a fundamental point of view, where Ti resides and how it helps to lower the hydrogen desorption temperature in sodium alanate $NaAlH_4$. Unfortunately, there is a continuing experimental controversy regarding the sites that Ti atoms occupy as well as the exact role of the catalyst in hydrogen sorption. For example, some suggest that Ti is substituted at the Na site[10,11] or the Al site[12] in the bulk while others find that Ti remains on the surface as a Ti-Al alloy.[13–20] Formation of Ti hydrides[21,22] or defects[12,23] has also been suggested by other experiments. On the other hand, the theoretical results are in agreement. Several authors[24–26] have calculated, using first principles theory, the sites Ti atoms would prefer to occupy, the changes in the electronic structure and the hydrogen bond strength as Ti replaces the Na or the Al site, and the energy necessary to remove a hydrogen atom. Taking the bulk cohesive energies of Ti, Na, and Al as reference, it is found that the least energetically unfavorable site for Ti to occupy is the Al site. In addition, the sub-surface Al site is more preferable than the bulk Al site.[25] The substitution of Ti atoms weakens the covalent bonds that hold the hydrogen atoms and thus lowers the desorption temperature of hydrogen irrespective of which metal sites the Ti atoms occupy.[27]

Studies of hydrogen desorption from sodium-aluminum hexahydride Na_3AlH_6, however, is limited. Experiments[28,29] have been carried out by directly doping Na_3AlH_6 with Ti. It is found that mechanically alloyed Na_3AlH_6 exhibits faster kinetics than Na_3AlH_6 obtained from the decomposition of $NaAlH_4$. Kiyobayashi *et al.*[28] reported that Na_3AlH_6 presents an equal dehydrogenation rate compared to $NaAlH_4$ upon Ti doping over the temperature range 363–423 K, while Kircher and Fichtner[29] found that Na_3AlH_6 decomposes more slowly than $NaAlH_4$ in the first step of the reaction in Eq. (1) below the temperature of 423 K. The theoretical calculations[9,30] on Na_3AlH_6 are limited to the studies of electronic band structure and lattice dynamics. No calculations, to our knowledge, have been carried out to see what sites Ti atoms occupy or what role it plays in the hydrogen desorption. In this paper we concentrate on this issue. Using first principles theory we have studied the structural and elec-

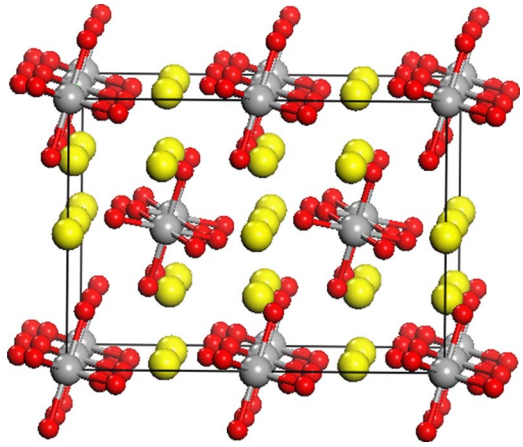

FIG. 1. (Color online) The 80-atom supercell geometry of $Na_{24}Al_8H_{48}$ is illustrated above. The yellow (light gray), gray, and red (dark gray) atoms correspond to Na, Al, and H, respectively.

tronic properties of Na_3AlH_6 and compared these with earlier calculations and experiments. We then determined the sites Ti atoms would prefer by comparing the total energies of various supercells where Ti is substituted at the Na and Al sites. The energy necessary to remove a H atom from pure Na_3AlH_6 is compared to that when Ti is substituted at the Na or Al site to determine the role of Ti on hydrogen desorption. We have also investigated the role of Na and Al vacancies on the hydrogen removal energy.

In Sec. II we describe our theoretical procedure. The results are discussed in Sec. III and summarized in Sec. IV.

II. THEORETICAL METHOD

The calculations are based on density-functional theory (DFT) (Ref. 31) and the Perdew-Wang prescription for the generalized gradient approximation (GGA) (Ref. 32) for the exchange and correlation potential. The atomic energies of H and Ti atoms were calculated using the spin-polarized density functional theory as this is necessary to compute the correct binding energy of H_2 and the Ti atom. We used a $(2\times2\times1)$ supercell consisting of 80 atoms ($Na_{24}Al_8H_{48}$) to represent the Na_3AlH_6 lattice (see Fig. 1). To simulate the substitution of the Na site by Ti or to create a Na vacancy, we replaced the Na (0.5, 0.5, 0.5) site. For the substitution of Ti at the Al site or to create an Al vacancy, we used the Al (0.75, 0.25, 0.5) site. The optimization of the supercell with and without defects (substitutional Ti or vacancies) was performed using the Vienna *ab initio* Simulation Package (VASP).[33] We used the projector augmented plane wave (PAW) (Ref. 34) method with $2p$, $3s$ valence states for Na, $3s$ and $3p$ valence states for Al, and $1s$ valance state for H. The energy cutoff in the plane wave expansion was set at 800 eV.[9] Self-consistency in the total energy was obtained to an accuracy of 1 meV. The geometry of the supercell [ionic coordinates and (c/a) ratio] was optimized without symmetry constraint by calculating the Hellmann-Feynman forces on the atoms and stresses on the supercell. The Hellman-Feynman force components on each ion in the supercells were converged to 5 meV/Å. The irreducible wedge of the Brillouin zone was sampled using a k-point grid of $3\times3\times3$ for geometry optimization and $4\times4\times4$ for the density of states (DOS) calculation at the equilibrium volume. The DOS was calculated using the modified tetrahedral method of Blöchl *et al.*[35] The electron localization function (ELF) which provides a description of the bonding characteristics are calculated following the procedure outlined by Becke and Edgecombe.[36] We have studied the influence of temperature by carrying out molecular dynamics simulations (MD) at 300 K. One thousand time steps, each 1 fs long, were chosen for the equilibration. The velocities were scaled at each time step. We have neglected the effect of configuration entropy in our calculations. Recently, Watari *et al.*[37] calculated configuration entropy in Pd-hydrogen clusters and found it to be 0.05 eV. This small contribution will not affect our conclusions. In the following we present the results of these comprehensive calculations.

III. RESULTS AND DISCUSSIONS

A. Structure and electronic properties of Na_3AlH_6

Na_3AlH_6 has a monoclinic crystal structure with $P2_1/n$ symmetry. Here the Al atom occupies the $2a$ (0, 0, 0) site and is decorated with six H atoms forming a slightly distorted AlH_6 octahedron. The Na atoms occupy both $2b$ (0, 0, 0.5) and $4e$ (0.993, 0.461, 0.252) sites. The average distance between the Al and the H atoms is 1.76 Å which is slightly larger than that in $NaAlH_4$, namely, 1.63 Å.[38] In Table I, the calculated lattice constants and the various interatomic distances of Na_3AlH_6 are listed. These values agree well with recent experiments performed in the 100 and 160 °C temperature range.[39,40] We have also calculated the enthalpy of the reaction in Eq. (2). The resulting theoretical value of 48.6 KJ/mol/H_2 also agrees well with the experimental value of 47 KJ/mol/H_2 measured from temperature 199 to 244 °C.[41]

The electronic structure of Na_3AlH_6 is studied by examining both the partial and total density of states (Fig. 2) as

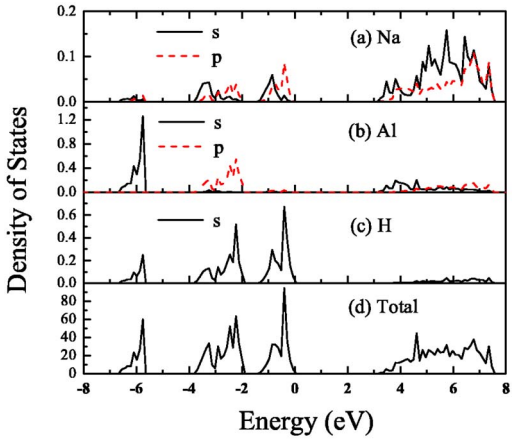

FIG. 2. (Color online) Density of states of $Na_{24}Al_8H_{48}$ supercells, the calculated s- and p- partial DOS of Na and Al and s-partial DOS of H in the $Na_{24}Al_{16}H_{64}$ supercell are shown in panels (a), (b), and (c) respectively. The total density of states is given in panel (d).

TABLE I. Comparison between experimental and theoretical values of lattice parameters and bond distances in intrinsic and Ti doped Na_3AlH_6 supercell.

	Theory $(1\times1\times1)$			Experiment $(1\times1\times1)$
	Intrinsic	Ti→Na	Ti→Al	Intrinsic
a	5.347	5.343	5.395	5.39,[a] 5.454[b]
b	5.526	5.473	5.564	5.514,[a] 5.547[b]
c	7.678	7.635	7.753	7.725,[a] 7.811[b]
β	89.92	89.81	89.98	89.86,[a] 89.83[b]
V	226.87	223.26	232.73	229.59,[a] 236.31[b]
Al-H	1.75–1.77			1.75–1.77[a]
Na-H	2.227 2.250 2.271			2.226[a] 2.261[a] 2.268[a]
Ti-H		1.99	1.85–1.86	

[a]Reference 39.
[b]Reference 40.

well as the electron localization function (Fig. 3). We see from the total density of states in Fig. 2(d) that Na_3AlH_6 is an insulator characterized by a band gap of 3.3 eV, which is 1.3 eV smaller than that of $NaAlH_4$.[42] Similar to $NaAlH_4$, the insulating behavior originates from ionic bonding between Na^+ and the Al-H complex. Different from $NaAlH_4$, the valence band is split into three regions instead of two. The low energy region is dominated by Al *s* and H *s* hybridized states and separated from the next band by an energy gap of ~2 eV. The next band located between −3.7 and −2.0 eV is composed of Al *p* and H *s* hybridized states, which indicates that the Al-H bond is covalent in nature. The top of the valence band is dominated by H *s* states and has a calculated bandwidth of 1.3 eV. Peles *et al.* [30] have mentioned that the top of the valance band is the result of the interaction between Al *d* and H *s* orbitals. Even though Al *d* states are not considered in our calculations, the calculated total DOS does not differ much from their results. The bottom of the conduction band just above the Fermi energy is primarily composed of the Na *s* and *p* antibonding states.

In Fig. 3(a) the electron localization function on the (001) plane of Na_3AlH_6 is plotted. One can observe the high ELF within the AlH_6 complex, which confirms the expected covalent bonding between Al and H atoms. The very low value of the ELF between Al-H complex and Na^+ reflects the ionic bonding between Na atoms and the nearest AlH_6 complexes.

B. Electronic structure and energetics of Ti substituted Na_3AlH_6

The substitution of Ti at the Na and Al sites in Na_3AlH_6 was investigated by considering $(TiNa_{23})Al_8H_{48}$ and $Na_{24}(TiAl_7)H_{48}$ supercells, respectively. With Ti replacing the Na site, the volume of the resulting lattice is smaller than that of the intrinsic Na_3AlH_6. Ti attracts one hydrogen atom from each of the six adjacent AlH_6 complexes and the corresponding Al-H bond distance is increased to 1.86 Å. Ti becomes octahedrally coordinated to H atoms with a bond distance of 1.99 Å. The Ti-H bond distance is much shorter than the original Na-H bond distance, thus causing the volume to decrease. On the other hand, upon substitution of Ti at the Al site, the volume of the resulting lattice is larger than that of the pure Na_3AlH_6 lattice. This enlargement arises because the Ti-H bond length of 1.85 Å is longer than the

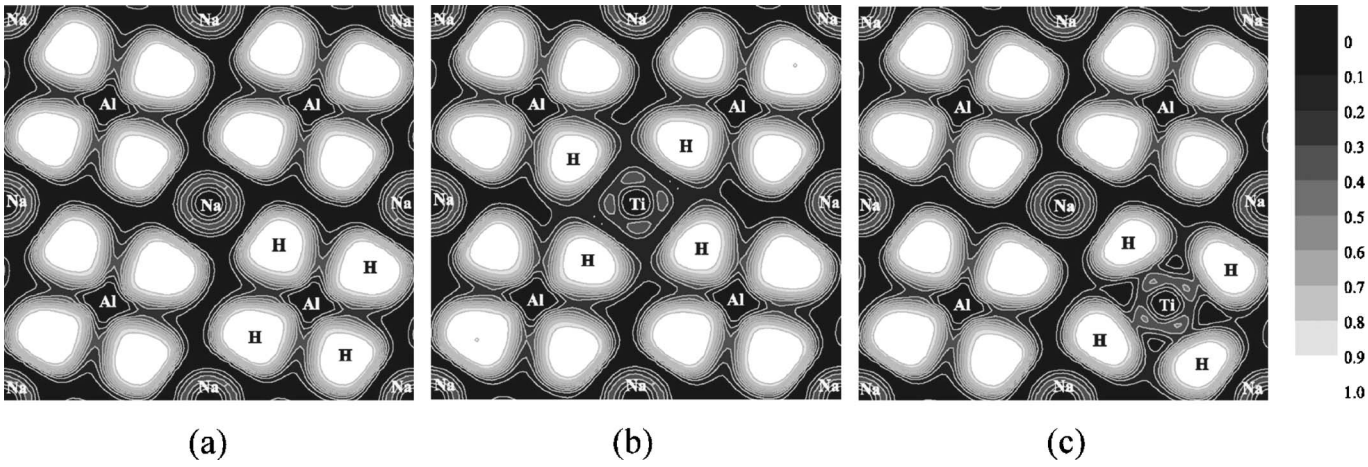

FIG. 3. Electron localization functions (ELF) on the (001) plane of (a) $Na_{24}Al_8H_{48}$, (b) $(TiNa_{23})Al_8H_{48}$, and (c) $Na_{24}(TiAl_7)H_{48}$ supercells.

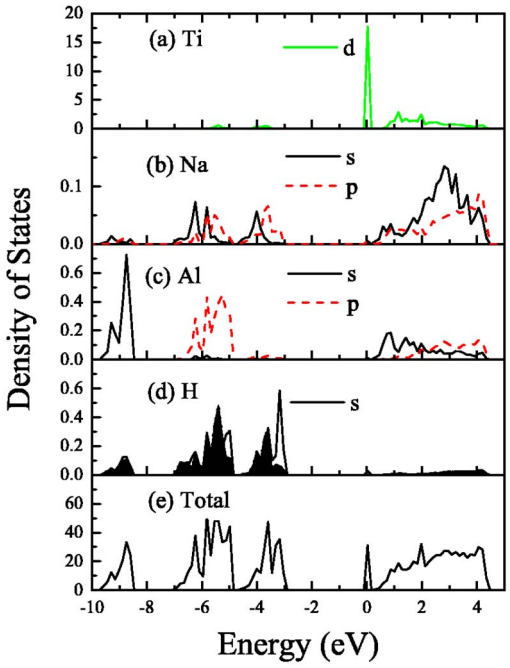

FIG. 4. (Color online) Density of states of $(TiNa_{23})Al_8H_{48}$ supercells, the calculated *d*-partial DOS of Ti, *s*- and *p*- partial DOS of Na and Al and *s*-partial DOS of H (adjacent to Ti and far away from Ti) are shown in panels (a), (b), (c), and (d), respectively. In panel (d), the region marked by black is the DOS of one of the H atoms adjacent to the Ti atom. The total density of states is given in panel (e).

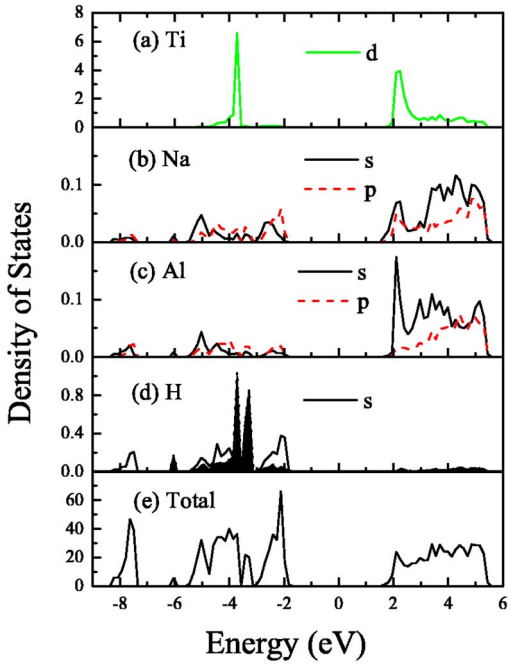

FIG. 5. (Color online) Density of states of $Na_{24}(TiAl_7)H_{48}$ supercells, the calculated *d*-partial DOS of Ti, *s*- and *p*- partial DOS of Na, and Al and *s*-partial DOS of H (adjacent to Ti and far away from Ti) in the supercell are shown in panels (a), (b), (c), and (d), respectively. In panel (d), the region marked by black is the DOS of one of the H atoms adjacent to the Ti atom. The total density of states is given in panel (e).

Al-H bond length of 1.76 Å. It should be emphasized that much of the changes occur within the single AlH_6 unit where the Al site is replaced by Ti. The structures of the other AlH_6 units remain mostly unaffected.

In Fig. 4 we plot the total and partial density of states (DOS) of the $(TiNa_{23})Al_8H_{48}$ supercell. Ti *d* states induce a sharp peak exactly at the Fermi level just below the conduction band. Ti *d* orbitals do not interact with H *s* orbitals. Therefore, they are nonbonding states. The total and partial density of states of $Na_{24}(TiAl_7)H_{48}$ supercell are plotted in Fig. 5. In contrast to the supercell where Ti was substituted at the Na site, Ti *d* orbitals in $Na_{24}(TiAl_7)H_{48}$ supercell split into e_g and t_{2g} orbitals under octahedral geometry. The Ti e_g orbitals then hybridize with H *s* orbitals to form bonding states, which give rise to the peak centered at −3.4 eV in the total density of states. Notice that the DOS due to the hydrogen atom adjacent to the Ti atom is totally different from other hydrogen atoms [see Fig. 5(d)]. It is mainly located in the middle of the valence band, i.e., between −3 and −6 eV and mixed with the Ti *d* states.

The ELF of $(TiNa_{23})Al_8H_{48}$ is shown in Fig. 3(b). Ti is found to attract one hydrogen atom from the adjacent Al-H complexes, but there is no directional covalent bond between the Ti and H atoms. In Fig. 3(c), on the other hand, we can see directional bonding between the Ti and H atoms, which indicates that the Ti *d* orbitals are coupled with the H *s* orbitals. Therefore, the Ti-H bond is mainly covalent.

To determine if Ti would occupy the Na or Al site, we calculate the substitution enthalpy using the following equation:

$$\Delta H = [E(\mathrm{Ti}_x\mathrm{Na}_y\mathrm{Al}_z\mathrm{H}_{48}) + (24-y)E(\mathrm{Na}_{\mathrm{bcc}}) + (8-z)E(\mathrm{Al}_{\mathrm{fcc}})] - [xE(\mathrm{Ti}_{\mathrm{hcp}}) + E(\mathrm{Na}_{24}\mathrm{Al}_8\mathrm{H}_{48})]. \quad (4)$$

Here the indices *x*, *y*, and *z* refer to the number of Ti, Na, and Al atoms. Note that the total energies calculated in the VASP code are referenced to the energies of the dissociated atoms. While some authors[24,43] have used the atomic energies as reference to compute ΔH and hence conclude which site is energetically preferable for Ti to occupy, others[25] have used the cohesive energies of Ti, Na, and Al for the computation of ΔH. Here we have used the latter as neither the Ti atoms introduced into the alanate nor the Na or Al atoms replaced exist as free atoms. We have computed the cohesive energies for hcp Ti, bcc Na, and fcc Al. These energies are 5.508, 1.102, and 3.489 eV/atom, respectively, and agree well with the corresponding experimental values of 4.85, 1.113, and 3.39 eV/atom.[44] The calculated binding energy for a H_2 molecule, namely, 4.562 eV also compares well with experimental value of 4.75 eV.[45] The energies calculated using Eq. (4) are listed in Table II. The positive values of the energies in the above equations imply that substitution is energetically unfavorable at 0 K. Note that the least unfavorable site for Ti

TABLE II. The enthalpy of formation (column 2) and hydrogen desorption energy from various supercells of Ti doped and vacancy containing Na_3AlH_6 (column 3). The negative entries in the third column suggest that the reaction is exothermic.

Super cell	Formation enthalpy (eV)	Hydrogen removal energy (eV)
$Na_{24}Al_8H_{48}$	0	1.461
$(TiNa_{23})Al_8H_{48}$	2.418	0.759
$Na_{24}(TiAl_7)H_{48}$	0.933	1.379
$Na_{23}Al_8H_{48}$	2.609	−1.452
$Na_{24}Al_7H_{48}$	3.669	−0.145[a]

[a]The energy to desorb a H_2 molecule.

is to occupy the Al site. This was also observed in the case of Ti doping in sodium alanate, $NaAlH_4$.[25]

To calculate the energy needed to remove a H atom from pure Na_3AlH_6 as well from those where Ti is substituted at the Na and the Al site, we have repeated the geometry optimization and total energy calculations of $Na_{24}Al_8H_{47}$, $TiNa_{23}Al_8H_{47}$, and $Na_{24}TiAl_7H_{47}$ supercells, respectively. The hydrogen removal energies are calculated using the following equation:

$$E^{\mathrm{H}} = E(\mathrm{Ti}_x\mathrm{Na}_y\mathrm{Al}_z\mathrm{H}_{48-n}) + n/2E(\mathrm{H}_2) - E(\mathrm{Ti}_x\mathrm{Na}_y\mathrm{Al}_z\mathrm{H}_{48}). \quad (5)$$

Positive values of the above energies imply that energy will be needed to remove a hydrogen atom whereas negative values imply that the reaction is exothermic. The results are also given in Table II. We see that the energy needed to remove a H atom from Na_3AlH_6 is 1.46 eV which is comparable to the energy needed to remove a H atom from $NaAlH_4$, namely, 1.68 eV.[42] These energies show that the Al-H bond is actually weaker in Na_3AlH_6 than that in $NaAlH_4$. When Ti occupies the Al site, the energy cost to remove hydrogen is still high, namely, 1.38 eV. This is because of the strong affinity of Ti to H. However, the hydrogen removal energy, namely, 0.76 eV, is reduced further when Ti replaces the Na site. This reduction is consistent with the resulting changes in the Al-H bonding: Following Ti substitution at the Na site, the H atom in its vicinity is not only bonded to Al but also to Ti. The longest Al-H bond distance in each AlH_6 complex in the vicinity of the Ti site in the $TiNa_{23}Al_8H_{64}$ supercell is 1.86 Å and the corresponding Ti-H bond distance is 1.99 Å. The Al-H bond distance in the *pure* Na_3AlH_6, on the other hand, is around 1.76 Å. Since elongation of a bond is associated with bond weakening, the energy to remove H is reduced. This is consistent with the role of Ti in hydrogen desorption in $NaAlH_4$.

We emphasize that the substitution of Ti at the Na site, although energetically less favorable, has a greater effect in promoting hydrogen desorption. The energy cost is reduced by nearly a factor of two than that from the pure Na_3AlH_6. The energy needed to remove a H atom from Ti substituted at the Al site is only marginally smaller than that from the pure hexahydride.

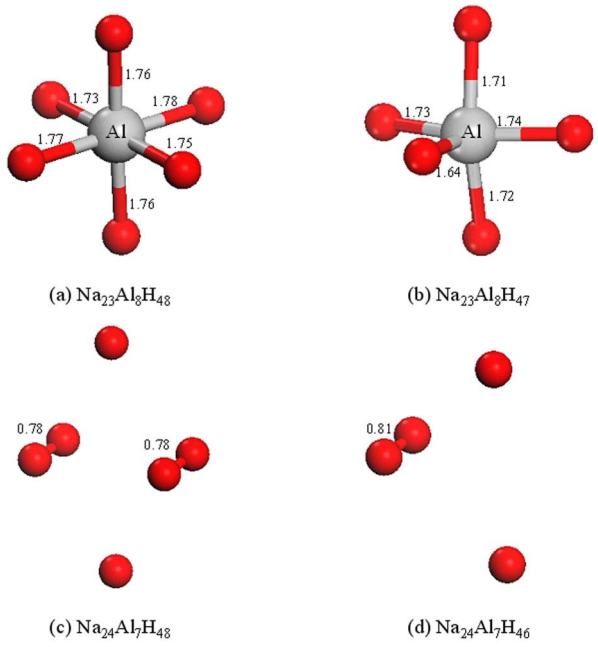

FIG. 6. (Color online) The geometries of the AlH_6 complexes in (a) $Na_{23}Al_8H_{48}$, AlH_5 in (b) $Na_{23}Al_8H_{47}$, supercells and those of H_6 and H_4 complexes in (c) $Na_{24}Al_7H_{48}$ and (d) $Na_{24}Al_7H_{46}$ supercells, respectively.

C. Role of Na and Al vacancies in hydrogen desorption

Recently the presence of point defects in ball milled samples of Ti-doped sodium alanate has been seen,[23] although the nature of these defects is not well established. No experiments are available to our knowledge that probe defects in Na_3AlH_6. However, we have examined the role that vacancy defects can play on hydrogen desorption by calculating the optimized geometry and total energies of $Na_{23}Al_8H_{48}$ and $Na_{24}Al_7H_{48}$ supercells. The former corresponds to the creation of a Na vacancy while the later corresponds to the creation of an Al vacancy. The geometries of each of these supercells were fully optimized as outlined before. In Figs. 6(a) and 6(c) we give the geometries of the AlH_6 complex in $Na_{23}Al_8H_{48}$ and $Na_{24}Al_7H_{48}$ following the creation of a Na and an Al vacancy, respectively. Note that while there are only minimal changes in the geometry of the AlH_6 complex following the creation of a Na vacancy, the changes are enormous when an Al vacancy is created. In this case, the nearest six hydrogen atoms form two hydrogen molecules with a bond distance of 0.78 Å, and the remaining two hydrogen atoms are bonded to the two nearest Na atoms with a bond distance of 2.1 Å. Molecular dynamics simulations at 300 K lead to the same results. As a hydrogen atom is removed from the AlH_6 complex in the $Na_{23}Al_8H_{48}$ supercell, the structure of the AlH_5 complex undergoes distortion [see Fig. 6(b)]. However, in the case of the $Na_{24}Al_7H_{48}$ supercell, hydrogen desorbs as a molecule and not as an atom.

To determine if it is energetically possible to create Na and/or Al vacancies, we have calculated the vacancy formation energy using the following equations:

$$\Delta H_{\mathrm{Na}} = [E(\mathrm{Na}_{23}\mathrm{Al}_8\mathrm{H}_{48}) + E(\mathrm{Na}_{\mathrm{bcc}})] - E(\mathrm{Na}_{24}\mathrm{Al}_8\mathrm{H}_{48}), \quad (6)$$

$$\Delta H_{Al} = [E(Na_{24}Al_7H_{48}) + E(Al_{fcc})] - E(Na_{24}Al_8H_{48}). \quad (7)$$

These values are also given in Table II. Note that it is energetically more favorable to create a Na vacancy than an Al vacancy. This is because removal of an Al atom disrupts the covalent bonding of six H atoms while removal of a Na atom only disrupts effectively *one* ionic bond. It is interesting to compare the energies necessary to create Na and Al vacancies in Na_3AlH_6 versus those in $NaAlH_4$. It has been shown earlier that the net cost in creating an Al vacancy in $NaAlH_4$ is smaller than that for creating a Na vacancy. The situation in Na_3AlH_6 is just the opposite. This can be understood by noting that in $NaAlH_4$ the creation of an Al vacancy leads to the formation of two H_2 molecules and the energy gain in this process offsets some of the energy cost necessary to create the Al vacancy. However, in Na_3AlH_6 only four of the H atoms combine to form H_2 molecules while the other two H atoms remain bound to neighboring Na in atomic form.

The energies needed to remove a H atom from the vicinity of a Na or Al vacancy has been calculated by considering the $Na_{23}Al_8H_{47}$ supercell and $Na_{24}Al_7H_{46}$ supercell, respectively, [see Eq. (2) for guidance]. These energies are given in column 3 of Table II. Note that the energies for both Na and Al vacancies are negative. This means that the removal of hydrogen from the vicinity of a Na or an Al vacancy will be exothermic. We need to emphasize that hydrogen desorption is in the form of a single hydrogen atom in the case of the Na vacancy but in the form of a hydrogen molecule in the case of the Al vacancy.

We found that it is much easier to remove *one* H atom than two H atoms from each Al-H complex in $Na_{23}Al_8H_{48}$. This is because the adjacent Na atoms transfer three electrons to stabilize the $(AlH_6)^{3-}$ unit. With the creation of a Na vacancy, there are only two electrons available to stabilize the nearest AlH_6 complex. Removal of one H atom will leave behind a $(AlH_5)^{2-}$ complex which is charge balanced and therefore quite stable.

IV. CONCLUSIONS

In summary, we have studied the electronic structure, stability, and dehydrogenation of Na_3AlH_6 following the doping of Ti atoms as well as the creation of metal vacancies by using supercell band-structure formalism and the gradient corrected density functional theory. For Ti doped Na_3AlH_6, the least unfavorable location of Ti is found to be the Al site. However, Ti substituted at the Al site only marginally facilitates hydrogen desorption. On the other hand, the substitution of Ti at the Na site, although energetically less favorable, enhances desorption of hydrogen more effectively than Ti substituted at the Al site. We note that the vacancies can promote hydrogen desorption better than when Ti becomes a substitutional impurity. Since the creation of vacancies is energetically less likely, they may not dominate the hydrogen desorption process. In particular, recent experiments[46,47] showed that ball milling sodium alanate with a small amount of Ti cluster improves sorption kinetics better than $TiCl_3$. This suggests that the formation of NaCl (which could be the signature for the existence of Na vacancies) is not critical for hydrogen desorption. Similarly, the formation of Al vacancy is energetically more costly than the formation of Na vacancy, it too may not be responsible for hydrogen desorption. Thus, Ti substituted at the Na site may be playing a larger role in improving hydrogen desorption. This is consistent with some recent experiments[21,22] where Ti hydrides were found to form during doping or hydrogenation. We recall that Ti attracts hydrogen atoms to form a TiH_x cluster irrespective of whether Ti substitutes the Na or the Al site. However, when the Ti atom is occupying the Al site, the Ti-H bond is stronger than that when it occupies the Na site. Thus, desorption of hydrogen from a TiH_x cluster with the Ti atom occupying the Na site is the most preferable pathway for hydrogen desorption.

ACKNOWLEDGMENTS

This work was supported in part by grants from the Department of Energy (DOE), Swedish Research Council (VR), and by the Swedish Foundation for International Cooperation in Research and Higher Education (STINT).

[1] B. Bogdanovic and M. Schwickardi, J. Alloys Compd. **253**, 1 (1997).
[2] S. Suda, Y. M. Sun, B. H. Liu, Y. Zhou, S. Morimitsu, K. Arai, N. Tsukamoto, M. Uchida, Y. Candra, and Z. P. Li, Appl. Phys. A: Mater. Sci. Process. **72**, 209 (2001).
[3] K. Miwa, N. Ohba, S. I. Towata, Y. Nakamori, and S. I. Orimo, Phys. Rev. B **69**, 245120 (2004).
[4] P. Chen, Z. T. Xiong, J. Z. Luo, J. Y. Lin, and K. L. Tan, Nature (London) **420**, 302 (2002).
[5] J. F. Herbst and L. G. Hector, Phys. Rev. B **72**, 125120 (2005).
[6] L. Schlapbach and A. Zuttel, Nature (London) **414**, 353 (2001).
[7] E. C. Ashby and P. Kobetz, Inorg. Chem. **5**, 1615 (1966).
[8] D. A. Dilts and E. C. Ashby, Inorg. Chem. **11**, 1230 (1972).
[9] X. Ke and I. Tanaka, Phys. Rev. B **71**, 024117 (2005).
[10] C. M. Jensen, R. Zidan, N. Mariels, A. Hee, and C. Hagen, Int. J. Hydrogen Energy **24**, 461 (1999).
[11] D. L. Sun, T. Kiyobayashi, H. T. Takeshita, N. Kuriyama, and C. M. Jensen, J. Alloys Compd. **337**, L8 (2002).
[12] M. Fichtner, P. Canton, O. Kircher, and A. Leon, J. Alloys Compd. **404**, 732 (2005).
[13] V. P. Balema, J. W. Wiench, K. W. Dennis, M. Pruski, and V. K. Pecharsky, J. Alloys Compd. **329**, 108 (2001).
[14] G. J. Thomas, K. J. Gross, N. Y. C. Yang, and C. Jensen, J. Alloys Compd. **330**, 702 (2002).
[15] C. Weidenthaler, A. Pommerin, M. Felderhoff, B. Bogdanovic, and F. Schuth, Phys. Chem. Chem. Phys. **5**, 5149 (2003).
[16] E. H. Majzoub and K. J. Gross, J. Alloys Compd. **356**, 363 (2003).

[17] B. Bogdanovic, M. Felderhoff, M. Germann, M. Hartel, A. Pommerin, F. Schuth, C. Weidenthaler, and B. Zibrowius, J. Alloys Compd. **350**, 246 (2003).
[18] J. Graetz, J. J. Reilly, J. Johnson, A. Y. Ignatov, and T. A. Tyson, Appl. Phys. Lett. **85**, 500 (2004).
[19] R. T. Walters and J. H. Scogin, J. Alloys Compd. **379**, 135 (2004).
[20] M. Felderhoff, K. Klementiev, W. Grunert, B. Spliethoff, B. Tesche, J. M. B. von Colbe, B. Bogdanovic, M. Hartel, A. Pommerin, F. Schuth, and C. Weidenthaler, Phys. Chem. Chem. Phys. **6**, 4369 (2004).
[21] V. P. Balema and L. Balema, Phys. Chem. Chem. Phys. **7**, 1310 (2005).
[22] P. Wang, X. D. Kang, and H. M. Cheng, J. Phys. Chem. B **109**, 20131 (2005).
[23] O. Palumbo, R. Cantelli, A. Paolone, C. M. Jensen, and S. S. Srinivasan, J. Phys. Chem. B **109**, 1168 (2005).
[24] J. Iniguez, T. Yildirim, T. J. Udovic, M. Sulic, and C. M. Jensen, Phys. Rev. B **70**, 060101(R) (2004).
[25] O. M. Lovvik and S. Opalka, Phys. Rev. B **71**, 054103 (2005).
[26] C. Moyses Araujo, R. Ahuja, P. Jena, and J. M. Osorio Guillen, Appl. Phys. Lett. **86**, 251913 (2005).
[27] C. M. Araujo, S. Li, R. Ahuja, and P. Jena, Phys. Rev. B **72**, 165101 (2005).
[28] T. Kiyobayashi, S. S. Srinivasan, D. L. Sun, and C. M. Jensen, J. Phys. Chem. A **107**, 7671 (2003).
[29] O. Kircher and A. Fichtner, J. Alloys Compd. **404**, 339 (2005).
[30] A. Peles, J. A. Alford, Z. Ma, L. Yang, and M. Y. Chou, Phys. Rev. B **70**, 165105 (2004).
[31] W. Kohn and L. J. Sham, Phys. Rev. **140**, A1133 (1965).
[32] J. P. Perdew, K. Burke, and M. Ernzerhof, Phys. Rev. Lett. **77**, 3865 (1996).
[33] G. Kresse and J. Furthmuller, Phys. Rev. B **54**, 11169 (1996).
[34] P. E. Blöchl, Phys. Rev. B **50**, 17953 (1994).
[35] P. E. Blöchl, O. Jepsen, and O. K. Andersen, Phys. Rev. B **49**, 16223 (1994).
[36] A. D. Becke and K. E. Edgecombe, J. Chem. Phys. **92**, 5397 (1990).
[37] N. Watari, S. Ohnishi, and Y. Ishii, J. Phys.: Condens. Matter **12**, 6799 (2000).
[38] B. C. Hauback, H. W. Brinks, C. M. Jensen, K. Murphy, and A. J. Maeland, J. Alloys Compd. **358**, 142 (2003).
[39] E. Ronnebro, D. Noreus, K. Kadir, A. Reiser, and B. Bogdanovic, J. Alloys Compd. **299**, 101 (2000).
[40] K. J. Gross, S. Guthrie, S. Takara, and G. Thomas, J. Alloys Compd. **297**, 270 (2000).
[41] B. Bogdanovic, R. A. Brand, A. Marjanovic, M. Schwickardi, and J. Tolle, J. Alloys Compd. **302**, 36 (2000).
[42] S. Li, R. Ahuja, C. M. Araujo, B. Johansson, and P. Jena (unpublished).
[43] J. Iniguez and T. Yildirim, Appl. Phys. Lett. **86**, 103109 (2005).
[44] C. Kittel, *Introduction to Solid State Physics*, 7th ed. (Wiley, New York, 1995).
[45] F. I. Silvera, Rev. Mod. Phys. **52**, 393 (1980).
[46] M. Fichtner, O. Fuhr, O. Kircher, and J. Rothe, Nanotechnology **14**, 778 (2003).
[47] B. Bogdanovic, M. Felderhoff, S. Kaskel, A. Pommerin, K. Schlichte, and F. Schuth, Adv. Mater. (Weinheim, Ger.) **15**, 1012 (2003).